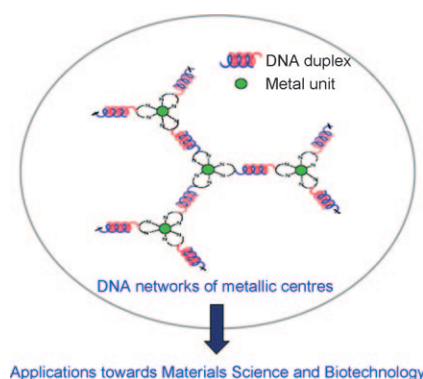


DNA goes nano! Ordered networks of metallic units based on DNA self-assembly (see figure) exhibit interesting functions and properties and are currently being developed for the fabrication of nanometer-scale devices.



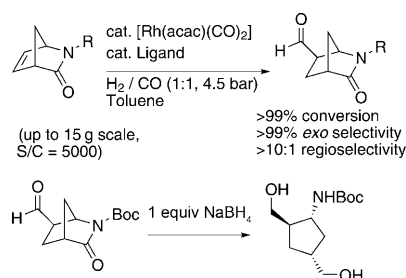
DNA Nanoarrays

*S. Ghosh, E. Defrancq** . . . 12780–12787

**Metal-Complex/DNA Conjugates:
A Versatile Building Block for DNA
Nanoarrays**

COMMUNICATIONS

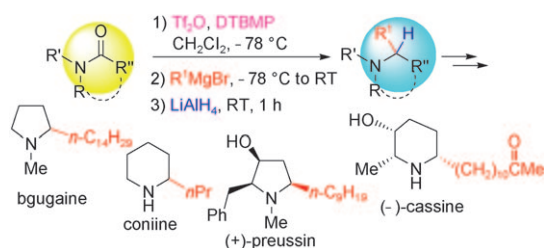
Customising a bicycle: Rh-catalysed asymmetric hydroformylation of a bicyclic lactam, 2-azabicyclo-[2.2.1]hept-5-en-3-one, was investigated. The use of a chiral diphosphite ligand, (*R,R*)-Kelliphite, enables excellent selectivity towards one regioisomer combined with excellent productivity and perfect *exo* selectivity. The products are versatile precursors to highly desired functionalised cyclopentylamines (see scheme).



Synthetic Methods

G. M. Noonan, C. J. Cogley, T. Lebl, M. L. Clarke** 12788–12791

Asymmetric Hydroformylation of an Enantiomerically Pure Bicyclic Lactam: Efficient Synthesis of Functionalised Cyclopentylamines



Direct entry: One-pot reductive alkylation of lactams/amides with Grignard reagents has been realized via lactam/amide activation with Ti_2O . This method opens a direct entry to α -alky-

lated amines. The versatility of the method is illustrated by the concise syntheses of bioactive alkaloids (\pm)-bgugaine, (\pm)-coniine, (+)-preussin, and ($-$)-cassine.

Alkaloids

*K.-J. Xiao, Y. Wang, K.-Y. Ye, P.-Q. Huang** 12792–12796

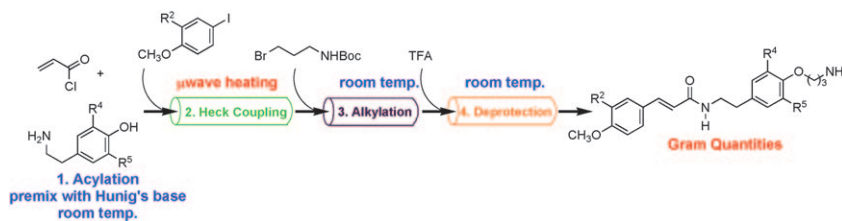
Versatile One-Pot Reductive Alkylation of Lactams/Amides via Amide Activation: Application to the Concise Syntheses of Bioactive Alkaloids (\pm)-Bgugaine, (\pm)-Coniine, (+)-Preussin, and ($-$)-Cassine



Synthetic Methods

S. Achanta, V. Liautard, R. Paugh,
M. G. Organ* 12797–12800

The Development of a General Strategy for the Synthesis of Tyramine-Based Natural Products by Using Continuous Flow Techniques



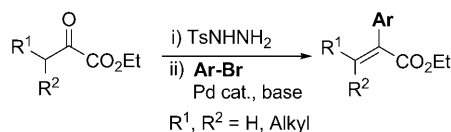
A flowing future! A multistep, general flow chemistry protocol has been developed for the preparation of tyramine-based natural products. The process integrates room-temperature reactions with high-temperature Heck coupling reactions, where the heat has

been supplied by microwave irradiation. As a proof of concept for 'scaling out' to attain larger quantities of the desired products, the four primary tyramine-based natural products were prepared on a gram scale using this synthetic protocol.

Cross-Coupling Reactions

J. Barluenga,* M. Tomás-Gamasa,
F. Aznar, C. Valdés* 12801–12803

Synthesis of 2-Arylacrylates from Pyruvate by Tosylhydrazide-Promoted Pd-Catalyzed Coupling with Aryl Halides



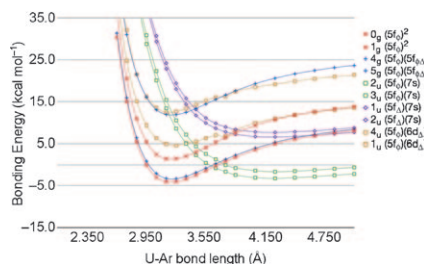
Important synthetic intermediates and direct precursors of the prophen class of anti-inflammatory agents, 2-arylacrylates are prepared in one step from ethyl pyruvate by employing the

recently developed Pd-catalyzed cross-coupling between tosylhydrazones and aryl halides. Moreover, substituted 2-oxoesters afford tri- and tetrasubstituted functionalized alkenes.

Noble Gas Matrices

I. Infante, L. Andrews, X. Wang,
L. Gagliardi* 12804–12807

Noble Gas Matrices May Change the Electronic Structure of Trapped Molecules: The UO₂(Ng)₄ [Ng = Ne, Ar] Case

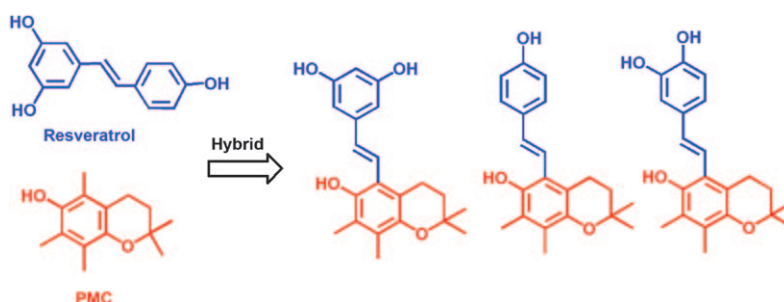


Ground state reversal from a neon to an argon matrix is confirmed by CASSCF/CASPT2 calculations (see picture) and new stepwise laser-ablated experiments.

Radical Scavengers

J. Yang, G.-Y. Liu, D.-L. Lu, F. Dai,
Y.-P. Qian, X.-L. Jin,
B. Zhou* 12808–12813

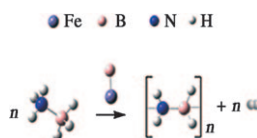
Hybrid-Increased Radical-Scavenging Activity of Resveratrol Derivatives by Incorporating a Chroman Moiety of Vitamin E



A winning combination: Resveratrol derivatives incorporating a chroman moiety of vitamin E were constructed, resulting in the remarkable enhancement in tris(2,4,6-trichloro-3,5-dinitrophenyl)methyl radical (HNTTM[•])-scavenging activity as compared with

the parent molecules (see scheme). Reaction kinetic analysis, oxidative product identification, and redox potential determination demonstrate that the reaction is governed by a sequential proton-loss electron-transfer (SPLET) mechanism.

Nano-alloy: Crystalline polyaminoborane is formed upon releasing 1.0 equiv-
alent H_2 from ammonia borane at
60 °C catalyzed by a nano-FeB alloy.
Our experimental results show that
about 1.0 and 1.5 equiv H_2 can be
released at 60 and 100 °C, respectively.



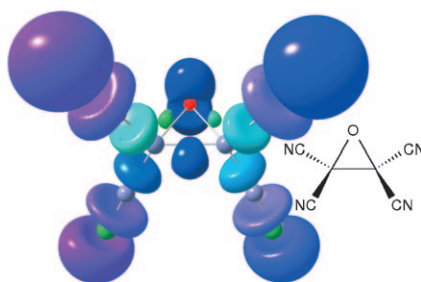
Heterogeneous Catalysis

*T. He, J. Wang, G. Wu, H. Kim,
T. Proffen, A. Wu, W. Li, T. Liu,
Z. Xiong, C. Wu, H. Chu, J. Guo,
T. Autrey, T. Zhang,
P. Chen** 12814–12817

**Growth of Crystalline Polyamino-
borane through Catalytic Dehydrogen-
ation of Ammonia Borane on FeB
Nanoalloy**



No longer hidden! An extension of the
capabilities of the X-ray diffraction
experiment is introduced. Locations of
electron pairs within a molecule can be
measured and made visible (see
figure). This is demonstrated on a
series of epoxides, for which ring
strain, crystal, and substituent effects
can be quantified. Comparison with
experimental and theoretical electron-
density analyses shows the advantages
of the new method.



Bond Theory

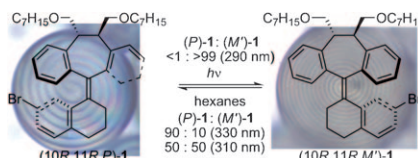
S. Grabowsky, D. Jayatilaka, S. Mebs,
P. Luger* 12818–12821

**The Electron Localizability Indicator
from X-Ray Diffraction Data—A First
Application to a Series of Epoxide
Derivatives**



FULL PAPERS

Doped for chirality: (10*R*,11*R*)-Di-
alkoxymethyldibenzosuberane-based
helicenes **1** with 7-bromo- α -tetralin-
type fragments were synthesized. Com-
plete switching selectivity (P/M' ,
<1 : >99) was observed in hexane
upon irradiation at 290 nm. The
reversed photoisomerization was also
achieved with high selectivity (P/M' ,
90:10) at 330 nm.

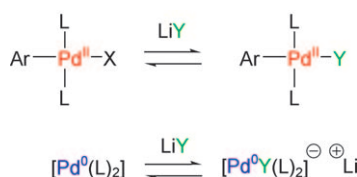


Liquid Crystals

*W.-C. Chen, P.-C. Lin, C.-H. Chen,
C.-T. Chen** 12822–12830

**Modulation of Photoswitching Profiles
by 10,11-Dialkoxymethyl Substituents
in C_2 -Symmetric Dibenzosuberane-
Based Helicenes**

Halides—one stone, two birds! An
unprecedented dual role of halide
anions in the Stille reaction has been
discovered. First halides can increase
or decrease the turnover-limiting trans-
metallation rate through in situ halide
metathesis (top equation). Second, hal-
ides stabilize the Pd^0 catalyst, prevent-
ing its decomposition, keeping the cat-
alyst loading in the catalytic cycle high
throughout the whole reaction (bottom
equation).



Homogeneous Catalysis

*S. Verbeek, C. Meyers, P. Franck,
A. Jutand,*
B. U. W. Maes** 12831–12837

**Dual Effect of Halides in the Stille
Reaction: In Situ Halide Metathesis
and Catalyst Stabilization**

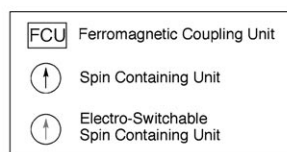
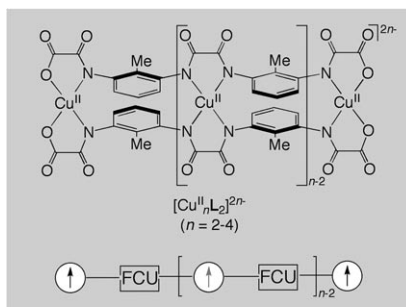


Molecular Wires

E. Pardo, J. Ferrando-Soria, M.-C. Dul, R. Lescouëzec, Y. Journaux,* R. Ruiz-García, J. Cano, M. Julve, F. Lloret,* L. Cañadillas-Delgado, J. Pasán, C. Ruiz-Pérez . . . 12838–12851



Oligo-*m*-phenyleneoxalamide Copper(II) Mesocates as Electro-Switchable Ferromagnetic Metal–Organic Wires



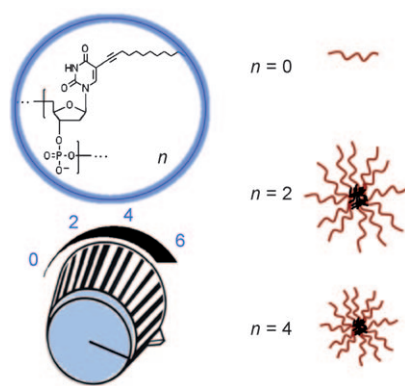
Down to the wire: The side-by-side self-assembly of a novel series of linear homo- and heterotopic oligo(2-methyl-1,3-phenyleneoxalamide) ligands by Cu^{II} ions leads to double-stranded di-, tri-, and tetranuclear copper(II) string complexes of *meso*-helicite type, which behave as effective electro-switchable metal–organic wires (see graphic).

Micellar Aggregates

M. Anaya, M. Kwak, A. J. Musser, K. Müllen,* A. Herrmann* 12852–12859



Tunable Hydrophobicity in DNA Micelles: Design, Synthesis, and Characterization of a New Family of DNA Amphiphiles



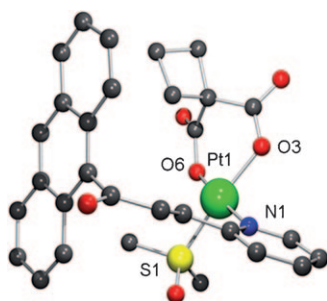
Tuning up the base: A strategy is proposed for tuning the size and stability of DNA-based micelle systems through precise incorporation of hydrophobic nucleobases. The effects of the positions and number of the modified nucleobases are investigated for a small family of such micelles (see picture).

Platinum Chemistry

P. Marqués-Gallego, J. Reedijk* 12860–12864



Unprecedented Water Addition to the α,β -Unsaturated Enone Bond, Mediated by the Combination of Carbonate and Platinum(II)



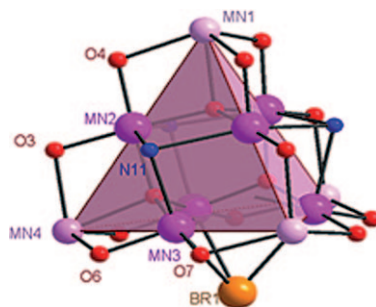
Test the water! The cytostatic compounds *cis*-[Pt(A9pyp)(dmsO)Cl₂] (**1**) and [Pt(A9pyp)(dmsO)(cbdca)] (**2**) (A9pyp = (*E*)-[1-(9-anthryl)-3-(2-pyridyl)-2-propenone] as carrier ligand; cbdca = cyclobutane dicarboxylate) have been found to add water across the enone C=C bond of the ligand A9pyp. The water addition occurs in the presence of carbonate buffer, and has been followed in detail using NMR spectroscopy and ESI-MS.

Cluster Compounds

S. Nayak, M. Evangelisti, A. K. Powell, J. Reedijk* 12865–12872

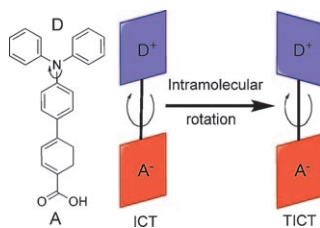


Magnetothermal Studies of a Series of Coordination Clusters Built from Ferromagnetically Coupled {Mn^{II}₄Mn^{III}₆} Supertetrahedral Units



Really cool clusters: Three structurally related mixed-valent polynuclear manganese complexes with supertetrahedral Mn₁₀ building blocks (an example is shown here) were prepared and magnetothermal analyses were performed. All the complexes possess very high ground-spin states and very small anisotropy. The magnetically isotropic nature of the complexes prompted the study of their magnetothermal properties.

To dye for: A series of organic dyes that feature a 1,3-cyclohexadiene conjugated moiety integrated into the π -conjugated framework has been synthesized and studied. Dye-sensitized solar cells based on these have shown appreciable conversion efficiency. Studies suggest the accessibility of the twisted internal charge-transfer state (TICT) in polar solvents (see figure).



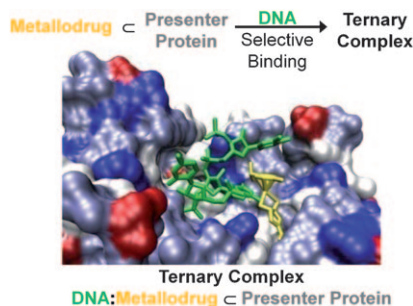
Energy Conversion

K.-F. Chen, C.-W. Chang, J.-L. Lin, Y.-C. Hsu, M.-C. P. Yeh, C.-P. Hsu,* S.-S. Sun** 12873–12882

Photophysical Studies of Dipolar Organic Dyes That Feature a 1,3-Cyclohexadiene Conjugated Linkage: The Implication of a Twisted Intramolecular Charge-Transfer State on the Efficiency of Dye-Sensitized Solar Cells



Match of the DNA: Chemo-genetic modifications of a ruthenium metallo-drug-presenter protein assembly (varying the complex or mutating the presenter protein) modulates the binding to different DNA targets (see figure).



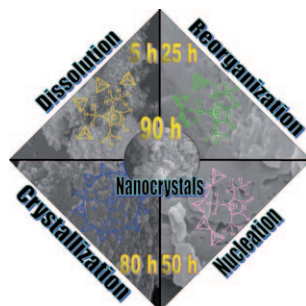
DNA Recognition

J. M. Zimbron, A. Sardo, T. Heinisch, T. Wohlschlager, J. Gradinaru, C. Massa, T. Schirmer, M. Creus,* T. R. Ward** 12883–12889

Chemo-Genetic Optimization of DNA Recognition by Metallo-drugs using a Presenter-Protein Strategy



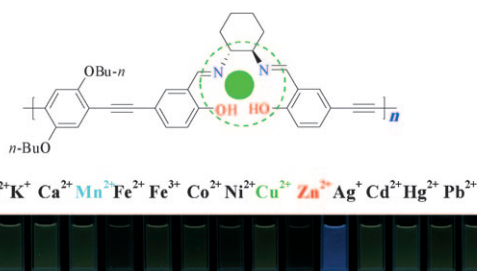
Growth control: Nucleation and growth processes of MnAlPO-5 nanosized crystals under ionothermal synthesis conditions are reported herein. Samples were examined at various stages of crystal growth of nanosized MnAlPO-5 under ionothermal conditions (see figure).



Ionic Liquids

*E.-P. Ng, L. Itani, S. S. Sekhon, S. Mintova** 12890–12897

Micro- to Macroscopic Observations of MnAlPO-5 Nanocrystal Growth in Ionic-Liquid Media



Sensing sensibility: A chiral polymer incorporating an (*R,R*)-salen moiety was synthesized and exhibits an excellent fluorescence response toward Zn^{2+} . The fluorescent color of the

polymer changed to bright blue instead of weak yellow after addition of Zn^{2+} , which could be easily detected by the naked eye (see picture).

Sensors

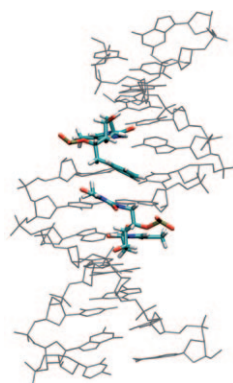
Y. Xu, J. Meng, L. Meng, Y. Dong, Y. Cheng, C. Zhu** 12898–12903

A Highly Selective Fluorescence-Based Polymer Sensor Incorporating an (*R,R*)-Salen Moiety for Zn^{2+} Detection



Nucleic Acids

*K. I. Shaikh, C. S. Madsen,
L. J. Nielsen, A. S. Jørgensen,
H. Nielsen, M. Petersen,
P. Nielsen* 12904–12919*

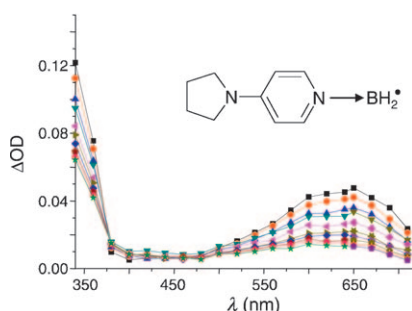


Communication in the minor groove: A series of aromatic moieties were inserted in the minor groove of DNA through 5'-(*S*)-*C*-substituted nucleosides. A strong and specific interaction was found between a thymine and a phenyl group in a crossed (–3)-zipper motif. Modelling revealed that the interaction is due to aromatic stacking across the minor groove (see figure).

Synthesis and Molecular Modelling of Double-Functionalised Nucleosides with Aromatic Moieties in the 5'-(*S*)-Position and Minor Groove Interactions in DNA Zipper Structures

Boranes

J. Lalevée, N. Blanchard,*
M.-A. Tehfe, A.-C. Chany,
J.-P. Fouassier 12920–12927*

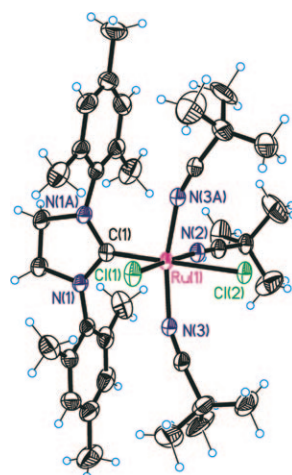


Radical thoughts: New N-heteroaryl boranes that exhibit low B–H bond-dissociation energy (BDE) are presented; excellent hydrogen-transfer properties have been found. Both the generation and the reactivity of the associated boryl radicals have been investigated through the direct detection of the different boryl radicals by laser flash photolysis (see graph).

New Boryl Radicals Derived from N-Heteroaryl Boranes: Generation and Reactivity

Ring-Opening Polymerization

*D. Wang, K. Wurst,
M. R. Buchmeiser* 12928–12934*

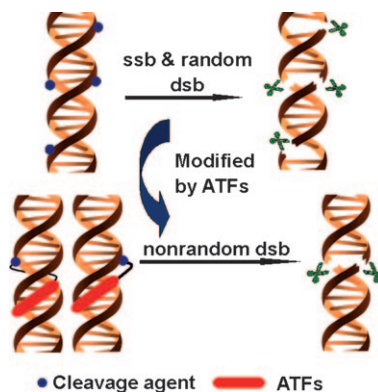


ROMPing around: A series of cationic and neutral Ru^{II} complexes based on N-heterocyclic carbenes have been synthesized and investigated for use as latent initiators for the photoinitiated ROMP by using different norborn-2-ene- and *cis*-cyclooctene-based monomers.

Cationic versus Neutral Ru^{II}–N-Heterocyclic Carbene Complexes as Latent Precatalysts for the UV-Induced Ring-Opening Metathesis Polymerization

DNA Cleavage

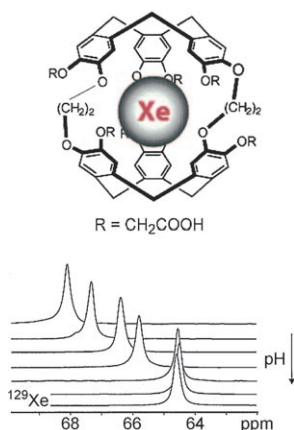
*C. Li, C. Du, H. Tian, C. Jiang, M. Du,
Y. Liu, R.-Z. Qiao,* Y.-X. Jia,*
Y.-F. Zhao* 12935–12940*



A new family of artificial transcription factor-based conjugates is designed and evaluated as effective double-strand DNA cleavage agents. When modified by polyamide, some non-selective and random cleavage agents were restricted within narrow limits when they interacted with double-strand DNA. These results are not only applicable to hydrolytic cleavage, but also to oxidative cleavage.

Artificial Transcription Factors which Mediate Double-Strand DNA Cleavage

(Xe)ing is believing! The interaction of hyperpolarized xenon with two water-soluble cryptophanes reveals interesting sensing properties. The presence of ionic substituents on the aromatic rings of the cage molecules renders the chemical shift of encapsulated xenon dependent on pH (see figure). When the ionic groups are, however, closer to the cavity portals, the nature of the counterion influences both the thermodynamics and the kinetics of the xenon binding.

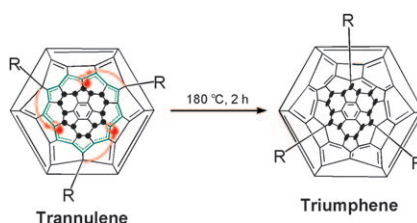


Sensors

P. Berthault, H. Desvaux, T. Wendlinger, M. Gyejacquot, A. Stopin, T. Brotin, J.-P. Dutasta, Y. Boulard* 12941–12946

Effect of pH and Counterions on the Encapsulation Properties of Xenon in Water-Soluble Cryptophanes

Colorful dance: A new class of compounds named “triumphenes” has been generated from trannulenes through an unprecedented migration of three organic addends (see figure).

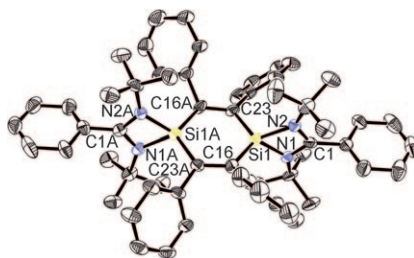


Fullerene Chemistry

E. A. Khakina, S. I. Troyanov, A. S. Peregudov, I. V. Soulimenkov, N. V. Polyakova, P. A. Troshin* 12947–12955

The Remarkable Chemistry of Trannulenes: Green Fluorinated Fullerenes with Unconventional Aromaticity

The new radicals: A novel amidinate-stabilized singlet delocalized biradicaloid [LSi(μ₂-C₂Ph₂)₂SiL] (L = PhC-(N*t*Bu)₂) has been synthesized successfully by the reaction of [PhC-(N*t*Bu)₂Si]₂ with diphenylacetylene. X-ray crystallography and DFT calculations show that the diradicals are stabilized by the amidinate ligand and the delocalization within the Si(μ₂-C₂Ph₂)₂Si six-membered ring (see figure).

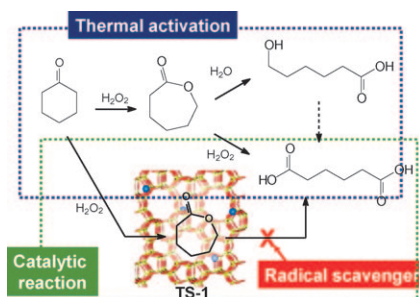


Silicon Chemistry

*H.-X. Yeong, H.-W. Xi, K. H. Lim, C.-W. So** 12956–12961

Synthesis and Characterization of an Amidinate-Stabilized *cis*-1,2-Disilylenylethene [*cis*-LSiC(Ph)=C(H)SiL] and a Singlet Delocalized Biradicaloid [LSi(μ₂-C₂Ph₂)₂SiL]

Oxidation control: In the oxidation of cyclohexanone with hydrogen peroxide under conditions aimed at obtaining ε-caprolactone, a thermally activated radical reaction leads to the concurrent formation of adipic acid (see figure). The relevant reaction rates are modified when Ti-silicalite is used as catalyst. The proper choice of solvent, which may also act as a radical scavenger, also allows control over the reaction rates.



Baeyer–Villiger Oxidation

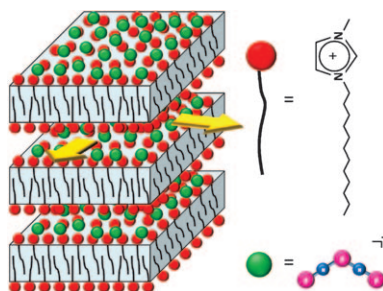
F. Cavani, K. Raabova, F. Bigi, C. Quarantelli* 12962–12969

A Rationale of the Baeyer–Villiger Oxidation of Cyclohexanone to ε-Caprolactone with Hydrogen Peroxide: Unprecedented Evidence for a Radical Mechanism Controlling Reactivity

Ionic Liquid Crystals

F. Xu, K. Matsumoto,*
R. Hagiwara 12970–12976

Effects of Alkyl Chain Length on Properties of 1-Alkyl-3-methylimidazolium Fluorohydrogenate Ionic Liquid Crystals

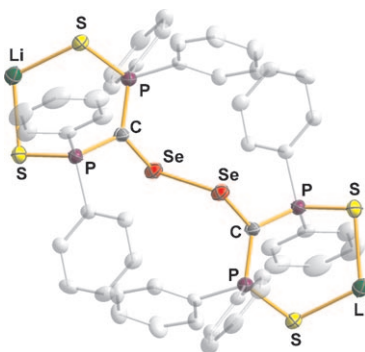


Ion-conductive layer: The $(\text{FH})_2\text{F}^-$ salts combined with 1-alkyl-3-methylimidazolium cations with long alkyl chains show smectic A_2 liquid crystalline mesophases. Highly anisotropic conductivity was observed in the smectic layer structure (see graphic).

Chalcogen Dimers

J. Konu, T. Chivers,*
H. M. Tuononen 12977–12987

Synthesis and Redox Behaviour of the Chalcogenocarbonyl Dianions $[(\text{E})\text{C}(\text{PPh}_2\text{S})_2]^{2-}$: Formation and Structures of Chalcogen–Chalcogen Bonded Dimers and a Novel Selone

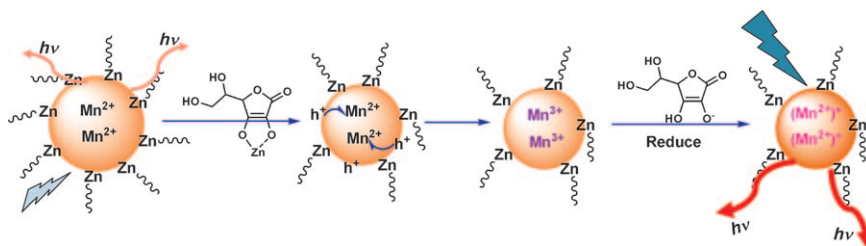


Versatility in chalcogenides: Tetradentate dimeric dianions $[(\text{SPh}_2\text{P})_2\text{CEEC}(\text{PPh}_2\text{S})_2]^{2-}$ ($\text{E} = \text{S}, \text{Se}$) with long, central chalcogen–chalcogen bonds (see figure) are formed by one-electron oxidation of the tridentate monomers $[(\text{E})\text{C}(\text{PPh}_2\text{S})_2]^{2-}$. Two-electron oxidation of $[\text{SeC}(\text{PPh}_2\text{S})_2]^{2-}$ produces the neutral selone $[(\text{Se})\text{C}(\text{PPh}_2\text{S})_2]$ as a LiI adduct.

Sensors

H.-F. Wang, Y. Li, Y.-Y. Wu, Y. He,
X.-P. Yan* 12988–12994

Ascorbic Acid Induced Enhancement of Room Temperature Phosphorescence of Sodium Tripolyphosphate-Capped Mn-Doped ZnS Quantum Dots: Mechanism and Bioprobe Applications



Vitamin see: The chelating ability of ascorbic acid (AA) enables the extraction of Mn and Zn from the surface of tripolyphosphate-capped Mn-doped ZnS quantum dots (QDs) generating more holes that are subsequently trapped by Mn^{2+} . The reducing property of AA results in the reduction of Mn^{3+}

to Mn^{2+} in an excited state, thus enhancing the excitation and orange emission of the QDs (see scheme). Such AA-induced phosphorescence enhancement enables selective detection of AA with a detection limit of 9 nM.

* Author to whom correspondence should be addressed

VIP Full Papers labeled with this symbol have been judged by two referees as being “very important papers”.

Supporting information on the WWW (see article for access details).

Video A video clip is available as Supporting Information on the WWW (see article for access details).

SERVICE

Spotlights 12774 Author Index 12996 Keyword Index 12997 Preview 12999

Issue 42/2010 was published online on October 28, 2010